

# Very deep X-ray observations of the anomalous X-ray pulsar 4U 0142+614

N. Rea,<sup>1★</sup> E. Nichelli,<sup>2,3</sup> G. L. Israel,<sup>2</sup> R. Perna,<sup>4</sup> T. Oosterbroek,<sup>5</sup> A. N. Parmar,<sup>6</sup>  
R. Turolla,<sup>7</sup> S. Campana,<sup>8</sup> L. Stella,<sup>2</sup> S. Zane<sup>9</sup> and L. Angelini<sup>10</sup>

<sup>1</sup>*SRON – Netherlands Institute for Space Research, Sorbonnelaan 2, 3584 CA, Utrecht, the Netherlands*

<sup>2</sup>*INAF – Astronomical Observatory of Rome, Via Frascati 33, 00040 Monteporzio Catone (Rome), Italy*

<sup>3</sup>*Dublin Institute for Advanced Studies, 5 Merrion Square, Dublin 2, Ireland*

<sup>4</sup>*JILA and Department of Astrophysical and Planetary Sciences, University of Colorado, 440 UCB, Boulder 80309, USA*

<sup>5</sup>*Science Payload and Advanced Concepts Office, ESA, ESTEC, Postbus 299, 2200 AG Noordwijk, the Netherlands*

<sup>6</sup>*Research and Scientific Support Department of ESA, ESTEC, Postbus 299, 2200 AG Noordwijk, the Netherlands*

<sup>7</sup>*University of Padua, Physics Department, via Marzolo 8, 35131 Padova, Italy*

<sup>8</sup>*INAF – Astronomical Observatory of Brera, via Bianchi 46, 23807 Merate (Lc), Italy*

<sup>9</sup>*Mullard Space Science Laboratory, University College London, Holmbury St Mary, Dorking Surrey RH5 6NT*

<sup>10</sup>*NASA, Goddard Space Flight Center, Greenbelt, MD, USA*

Accepted 2007 July 23. Received 2007 July 23; in original form 2007 February 28

## ABSTRACT

We report on two new *XMM–Newton* observations of the anomalous X-ray pulsar (AXP) 4U 0142+614 performed in 2004 March and July, collecting the most accurate spectrum for this source. Furthermore, we analyse two short archival observations performed in 2002 February and 2003 January in order to study the long-term behaviour of this AXP. 4U 0142+614 appears to be relatively steady in flux between 2002 and 2004, and the phase-averaged spectrum does not show any significant variability between the four epochs. We derive the deepest upper limits to date on the presence of lines in 4U 0142+614 spectrum as a function of energy: equivalent width in the 1–3 keV energy range  $<4$  and  $<8$  eV for narrow and broad lines, respectively. A remarkable energy dependence in both the pulse profile and the pulsed fraction is detected, and consequently pulse–phase spectroscopy shows spectral variability as a function of phase. By making use of *XMM–Newton* and *INTEGRAL* data, we successfully model the 1–250 keV spectrum of 4U 0142+614 with three models, namely the canonical absorbed blackbody plus two power laws, a resonant cyclotron scattering model plus one power-law and two log-parabolic functions.

**Key words:** stars: magnetic fields – stars: neutron – pulsars: individual: 4U 0142+614 – X-rays: stars

## 1 INTRODUCTION

Anomalous X-ray pulsars (AXPs) form a restricted family of neutron star (NS) X-ray sources with properties quite different from those of other known classes of X-ray emitting NSs, in particular the radio pulsars. However, in the last few years evidence was gathered of a possible link between AXPs and another peculiar class of NSs: the soft gamma-ray repeaters (SGRs; see Woods & Thompson 2006, for a recent review).

The nature of the strong X-ray emission from AXPs and SGRs is intriguing. In fact, their X-ray luminosity is too high to be powered by the loss of the star rotational energy alone, as in the more common

radio pulsars. At the same time, the lack of observational signatures of a companion strongly argues against an accretion powered binary system, favouring instead scenarios involving isolated NSs.

AXPs are usually radio-quiet and exhibit X-ray pulsations with spin periods in the  $\sim 5$ – $12$  s range. This, along with their large spin-down rates ( $\dot{P} \approx 10^{-13}$  to  $10^{-10}$  s s $^{-1}$ ), implies magnetic fields exceeding the (electron) critical magnetic field,  $B_{\text{cr}} \sim 4.4 \times 10^{13}$  G, if spin-down occurs mainly through magnetodipolar braking.

Furthermore, they are characterized by a high X-ray luminosity ( $L_X \approx 10^{34}$ – $10^{36}$  erg s $^{-1}$ ). Their high-energy emission ( $\sim 0.5$ – $100$  keV) is traditionally modelled by an absorbed blackbody ( $kT \sim 0.4$  keV) and two power laws ( $\Gamma_{\text{soft}} \sim 3$  and  $\Gamma_{\text{hard}} \sim 1$ ), although recently several attempts have been made to apply more physical spectral models (e.g. Perna et al. 2001; Rea et al. 2007a,b; Rea et al., in preparation).

★E-mail: n.rea@sron.nl

At present the model which appears most successful in explaining the peculiar observational properties of AXPs and SGRs is the ‘magnetar’ model. In this scenario AXPs and SGRs are thought to be isolated NSs endowed with ultrahigh magnetic fields ( $B \sim 10^{14} - 10^{15}$  G) the decay of which powers their X-ray emission (Duncan & Thompson 1992; Thompson & Duncan 1993, 1995, 1996). At magnetic fields higher than  $B_{\text{cr}}$ , radio emission is believed to be suppressed, e.g. by the photon-splitting process (Baring & Harding 1998), and this could explain why magnetars were believed not to show any radio emission. However, the discovery of radio pulsars with magnetic fields higher than the electron critical field (Camilo et al. 2000) and with very weak X-ray emission, as well as the discovery of radio pulsations from one magnetar (Camilo et al. 2006), is puzzling and still awaits explanation. Alternative scenarios, invoking accretion from a fossil disc, remnant of the supernova explosion (van Paradijs, Taam & van den Heuvel 1995; Chatterjee, Hernquist & Narayan 2000; Perna, Heyl & Hernquist 2000; Alpar 2001), encounter increasing difficulties in explaining the data.

4U 0142+614 is one of the brightest AXPs known to date, and it was first detected by *Uhuru* in 1978 (Forman et al. 1978). However, mainly because of the presence of the accretion-powered binary pulsar RX J0146.9+6121 nearby, only in 1994 was an  $\sim 8$ -s periodicity reported using *EXOSAT* data taken in 1984 (Israel, Mereghetti & Stella 1994). Long-term spin-period variations were discovered thanks to a large *RXTE* campaign (Gavriil & Kaspi 2002), leading to the measure of the period derivative  $\dot{P} \sim 2 \times 10^{-12} \text{ s s}^{-1}$ . Despite deep searches (Israel et al. 1994; Wilson et al. 1999), no evidence for orbital motion has been found, supporting the isolated NS scenario.

Further observations (White et al. 1987; Israel et al. 1999; Paul et al. 2000) revealed a soft (1–10 keV) X-ray spectrum typical of an AXP, best fitted by an absorbed blackbody ( $kT \sim 0.4$  keV) plus a power law ( $\Gamma \sim 3.7$ ). More recent *Chandra* (Juett et al. 2002; Patel et al. 2003), *XMM-Newton* (Göhler, Wilms & Staubert 2005) and *Swift* X-ray Telescope (XRT) (Rea et al. 2007a) observations have shown that 4U 0142+614 is a relatively stable X-ray emitter.

In the last few years, two peculiar characteristics of 4U 0142+614, have been found in comparison with other AXPs: (i) an optical counterpart (Hulleman, van Kerkwijk & Kulkarni 2000), displaying  $\sim 8$ -s pulsation with a 30 per cent pulsed fraction (Kern & Martin 2001)<sup>1</sup> and (ii) mid-infrared emission, tentatively interpreted as the signature of a non-accreting disc around the NS (Wang, Chakrabarti & Kaplan 2006). Furthermore, like in other AXPs, a hard X-ray emission up to 250 keV has been revealed (den Hartog et al. 2006; Kuiper et al. 2006; den Hartog et al. 2007).

In this paper we report on two new *XMM-Newton* observations of the AXP 4U 0142+614 performed in 2004 March and July. These observations provide by far the most accurate data collected in the soft X-ray band for this source. Furthermore, in order to study the long-term X-ray activity of 4U 0142+614 we analysed two archival observations (one of them already published by Göhler et al. 2005). Data analysis and results are presented in Section 2, while Section 3 deals with the spectral modelling of the 1–250 keV spectrum of 4U 0142+614. Finally our results are discussed in Section 4.

<sup>1</sup> Note that the detection of the optical counterpart to this object might be due to its lower extinction with respect to other AXPs, rather than to an intrinsic peculiarity.

## 2 OBSERVATIONS, DATA ANALYSIS AND RESULTS

4U 0142+614 has been observed with *XMM-Newton* four times, the first two times for a very short exposure time ( $\sim 6$  ks), while the last two observations are much deeper. These two very deep observations have been performed on 2004 March 1 and July 25, with on-source exposure times of 46 and 23 ks, respectively (see the end of this section for further details on the first two short observations). The *XMM-Newton Observatory* (Jansen et al. 2001) includes three 1500 cm<sup>2</sup> X-ray telescopes with an EPIC instrument in each focus, a reflecting grating spectrometer (RGS; den Herder et al. 2001) and an optical monitor (Mason et al. 2001). Two of the EPIC imaging spectrometers use MOS CCDs (Turner et al. 2001) and one uses a pn CCD (Strüder et al. 2001).

Data have been processed using SAS version 7.0.0, and we have employed the most updated calibration files available at the time the reduction was performed (2006 November). Standard data screening criteria are applied in the extraction of scientific products. We have cleaned the 2004 March observation for solar flares (the observation in July is not affected); the exposure time after the solar flare filtering is 37 ks.

Both 2004 observations have the same instrument set-up. pn and MOS1 cameras are used with the medium filters, while the thick filter is applied for the MOS2 camera. The pn camera is set in timing mode in order to avoid pile-up, the MOS1 with the central CCD in timing mode, and the others in prime full window mode. The MOS2 CCDs are all set in prime full window mode, with the aim of unveiling possible transient X-ray sources which might contaminate the instruments observing in timing mode. No transients are present in the MOS2 image. The source is, as expected, highly affected by pile-up. Hence, we do not consider the MOS2 data any further.

In order to extract more than 90 per cent of the source counts, we have constructed, for the data obtained with the pn and the MOS1 central CCD, a 1D image and we fit a Gaussian to the 1D photon distribution. We have then extracted the source photons from a rectangular region with RAWX and RAWY coordinates 37 100.75 and 18 197.5. The background is obtained from a rectangular region of the same size, as far as possible from the source, on the east side. Only photons with PATTERN  $\leq 4$  are used for the pn and with PATTERN  $\leq 12$  for the MOS1.

From the same regions we have extracted the 4U 0142+614 spectra. All of the EPIC spectra have been rebinned before fitting, so as to have at least 40 counts per bin and not to oversample the energy resolution by more than a factor of 3. We have also extracted first- and second-order RGS1 and RGS2 spectra for both source and background, using the standard procedure reported in the *XMM-Newton* analysis manual.

Thanks to the high timing and spectral resolution<sup>2</sup> of the pn (0.03 ms and  $E/\delta E \sim 50$ ) and MOS cameras (1.5 ms and  $E/\delta E \sim 50$ ), and to the high spectroscopical accuracy of the RGS ( $E/\delta E \sim 400$ ), we are able to perform timing and spectral analysis, as well as pulse-phase spectroscopy. The RGS spectra do not show evidence for narrow spectral features, and its continuum spectra are in good agreement with those of the pn and MOS1. We then do not report further on RGS data and refer to Durant & van Kerkwijk (2006a,b) for details on those. Furthermore, both MOS1 and pn give consistent timing and spectral results. Hence, we report hereafter

<sup>2</sup> See <http://xmm.esac.esa.int/> for details.

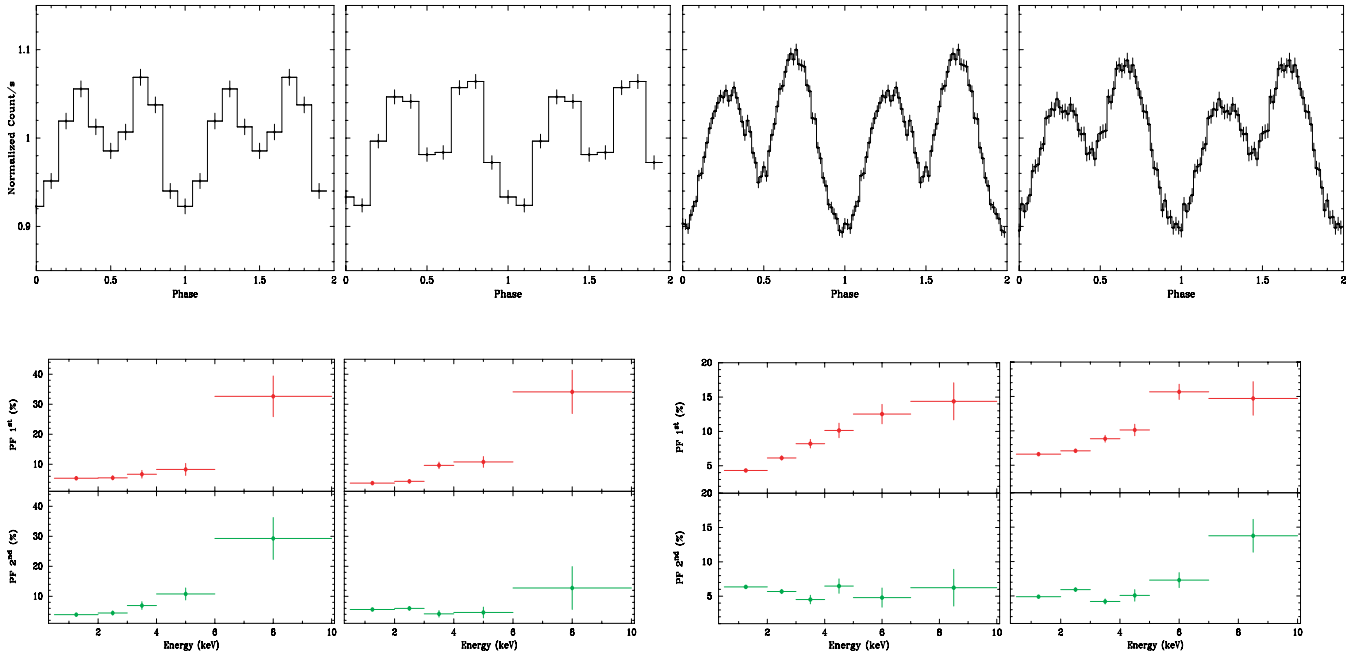


**Figure 1.** Top row: 0.3–10 keV background-subtracted pulse profiles of all the four *XMM–Newton* observations of 4U 0142+614. Bottom row: pulsed fraction as a function of energy for all the four *XMM–Newton* observations of 4U 0142+614. The top and bottom panels report, respectively, on the pulsed fraction (as defined in the text) of the fundamental and first harmonic sine functions which best fit the pulse profile of each observation (note that first two and last two panels from left-hand side have different y-axis units). For both top and bottom rows, the relative observations are (from left- to right-hand side): 2002 February, 2003 January, 2004 March and 2004 July.

only on the pn data. We find a pn (background-subtracted) count rate of  $46.2 \pm 0.1$  and  $46.5 \pm 0.1$  count  $s^{-1}$  for the 2004 March and July observation, respectively.

Furthermore, we have also analysed two short (6-ks exposure time each) *XMM–Newton* observations performed on 2002 February 13 and 2003 January 24 (the latter already reported in detail by Göhler et al. 2005). In both observations the pn camera is set up in small window mode. We use only pn data for these observations, and refer to Göhler et al. (2005) for details on MOS data for the 2003 January observation (MOS cameras gave results consistent with the pn for both observations). We have reprocessed and cleaned the data as reported above for the 2004 observations, resulting in an on-source exposure time in 2002 and 2003 of 2.0 and 3.5 ks, respectively. Thanks to the 2D image provided by the pn in small window mode, we have extracted the source events and spectra from a circular region of 25 arcsec around the 4U 0142+614 position. The background events and spectra, for both observations, are extracted from a similar circular region as for the source, although as far as possible (still within the central CCD) from the 4U 0142+614 position. The source pn count rate is  $42.1 \pm 0.5$  and  $40.5 \pm 0.6$  count  $s^{-1}$  for the 2002 February and 2003 January observations, respectively.

## 2.1 Timing analysis

In order to determine the spin period of 4U 0142+614, we have first corrected the event times to the barycentre of the Solar system (using the *SAS* tool *barycen*) and computed a power spectrum (*powspec*), where we find a strong signal around 8.6 s in all the observations. We use for the timing analysis only events in the 0.3–10 keV energy range. Timing analysis is performed using *Xronos*.

Two harmonics of the spin period are significantly detected in all four observations.

A precise estimate of the pulse period in the observations is obtained carrying out a period search (*efsearch*) around the 8.6 s value. We have then refined the period determination by dividing each observation into six intervals, and performing a linear fit to the phase determined in each interval (phase-fitting technique).

We obtain a best spin period of  $P_s = 8.6887(3)$  s (MJD 52318.0),  $P_s = 8.6882(2)$  s (MJD 52663.0),  $P_s = 8.68856(1)$  s (MJD 53065.0) and  $P_s = 8.688575(2)$  s (MJD 53211.0), for the *XMM–Newton* observations from 2002 February to 2004 July.<sup>3</sup> All these periods are consistent within their  $3\sigma$  errors with the more accurate *RXTE* timing analysis of this source (Dib, Kaspi & Gavril 2007).

The pulse profile of 4U 0142+614 is double peaked in all observations, and well modelled by two sine functions with periods fixed at the spin period and its first harmonic (see Fig. 1). Although the X-ray emission of 4U 0142+614 above 100 keV is completely pulsed (pulsed fraction of  $\sim 100$  per cent; Kuiper et al. 2006), in the soft X-rays 4U 0142+614 shows the smallest pulsed fraction of the class (a factor of  $\sim 3$  below that observed in other AXPs).

The pulsed fraction (defined as the semi-amplitude of the best-fitting fundamental sine function divided by the background corrected, constant level of the emission) in the 0.3–10 keV energy band is  $5.3 \pm 0.4$ ,  $5.9 \pm 0.4$ ,  $4.7 \pm 0.2$  and  $5.4 \pm 0.2$  per cent, from 2002 February to 2004 July. For a better comparison with previous results, we report also the peak-to-peak 0.3–10 keV pulsed fraction [defined as  $(F_{\max} - F_{\min}) / (F_{\min} + F_{\max})$ ], again from 2002 to 2004:  $8.8 \pm 0.9$ ,  $7.7 \pm 0.9$ ,  $10.2 \pm 0.2$  and  $13.3 \pm 0.3$  per cent.

<sup>3</sup> All errors in the text are reported at  $1\sigma$  confidence level, if not otherwise specified.

The 0.3–10 keV peak-to-peak pulsed fraction shows a modest ( $\sim 2.5\sigma$ ) increase between 2002 and 2004, possibly consistent with the evidence for a slow increase of the pulsed flux observed by *RXTE* (Dib et al. 2007). However, this is not followed by a similar increase of the fundamental sine-function pulsed fraction, which instead is within the errors relatively constant in time. This might be explained with the small changes of the pulse profile due mainly to the first harmonic of the signal, rather than to the fundamental.

Studying in detail the pulsed fraction as a function of energy, in all the observations, we find a peculiar pulsed fraction increase with energy: e.g. in 2004 March and July the fundamental pulsed fraction increases from about 4 to 15 per cent as the energy increases from 1 to 10 keV (see Fig. 1). Given the large errors on the pulsed fraction values in the 6–10 keV range for the 2002 February and 2003 January observations, this increase of the pulsed fraction with energy is consistent with having the same trend (within the errors) in all four observations. This effect was already hinted in other observations but the lower number of counts collected was not sufficient to reliably assess it (see e.g. fig. 5 of Israel et al. 1999; Paul et al. 2000; Göhler et al. 2005). It is worth noting that this trend cannot be an instrumental effect of the pn camera since the observations we report are taken in two different pn modes (small window and timing), and on the other hand this pulsed fraction increase was not observed in other AXPs or pulsars observed with the pn. Furthermore the presence of a hint of this increase also in *BeppoSAX* (Israel et al. 1999) and *ASCA* data (Paul et al. 2000) rule out any possible instrumental effect.

Correspondingly, the pulse profiles are highly variable with energy, as shown in Fig. 2. This variability of the pulse profile with energy has always been observed in this source (Israel et al. 1999; Paul et al. 2000; Patel et al. 2003; Morii, Kawai & Shibazaki 2005), as well as in other AXPs (see e.g. Mereghetti et al. 2004; Rea et al. 2005). To assess the statistical significance of these pulse profile variations, we have performed a Kolmogorov–Smirnov test on the energy resolved pulse profile for the 2004 March and July observations (see Fig. 2), and in both observations the difference between the soft (0.5–2 keV) and hard (7–10 keV) pulse profile is

highly significant, giving a probability that the profiles have the same shape smaller than  $10^{-6}$ . We have done the same test between the two observations to assess the pulse profile variability in time for a given energy range: in all the energy ranges the probability of the 2004 March and July profiles having the same shape is  $\sim 0.02$ , hence not very significant. However, note that *RXTE* monitoring over the last 10 yr did detect pulse profile variability with time, thanks to its higher sensitivity for pulse profile changes (Dib et al. 2007).

This increase with energy of the pulsed fraction of the fundamental component has not been observed so far in other AXPs, while the pulse profile change with energy is a more common behaviour (see e.g. Mereghetti et al. 2004; Woods et al. 2004; Rea et al. 2005).

## 2.2 Spectral analysis and pulse-phase spectroscopy

The phase-averaged spectra for all the observations are satisfactorily fitted by an empirical model consisting of an absorbed blackbody plus a power law ( $\chi^2_{\text{d.o.f.}} \simeq 1.0$ ; see Table 1 and Fig. 3). We use the XSPEC package (version 11.3 and 12.1) for all fittings, and used the phabs absorption model with the Anders & Grevesse (1989) solar abundances. A 2 per cent systematic error is included in all fits, as well as in the error calculation, to account for calibration uncertainties. Similarly to what has been done in the past for other AXPs, we have tried to fit the spectra of 4U 0142+614 with two absorbed blackbodies and with a Comptonized blackbody, but both trials resulted in a worse fit ( $\chi^2_{\text{d.o.f.}} > 2.4$ ). In all the observations the hydrogen column density is  $N_{\text{H}} \simeq 1 \times 10^{22} \text{ cm}^{-2}$ , and the absorbed flux in the 0.5–10 keV range is  $\sim 1.1 \times 10^{-10} \text{ erg cm}^{-2} \text{ s}^{-1}$ , corresponding to a luminosity of  $\sim 1 \times 10^{35} \text{ erg s}^{-1}$  (for a 3 kpc distance). In the 0.5–10 keV band, the blackbody component accounts for  $\sim 24$  per cent of the total absorbed flux. The blackbody radius, as derived from the fits, is smaller than the NS size. If the blackbody emission originates from the star surface, and is then partially upscattered to form the power-law component as predicted by the twisted magnetosphere model (see Sections 3

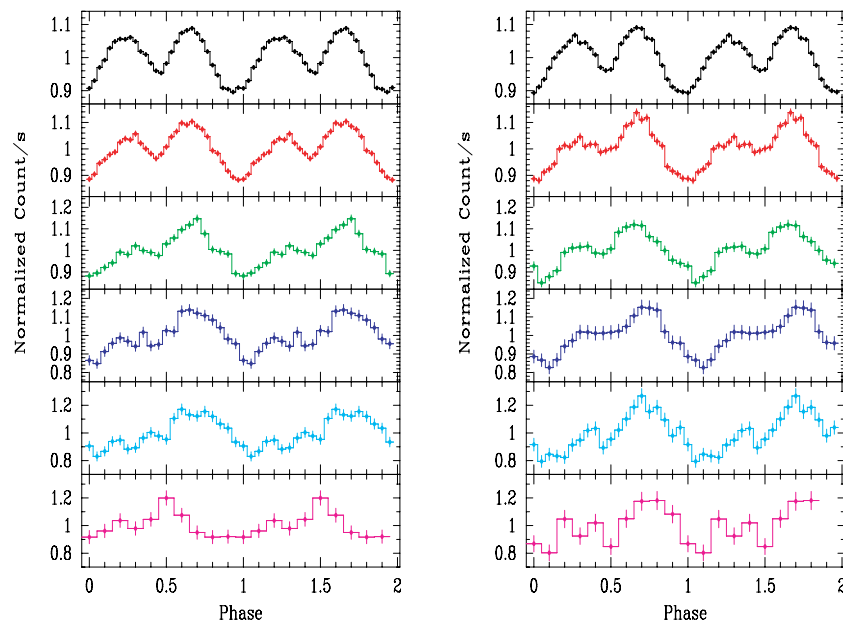


**Figure 2.** Epoch folding as a function of energy (from top to bottom: 0.5–2, 2–3, 3–4, 4–5, 5–7, 7–10 keV) for the 2004 March (left-hand panel) and July (right-hand panel) observations.

**Table 1.** Parameters of the spectral modelling of the 4U 0142+614 spectra with an absorbed blackbody plus a power law, for all the four XMM–Newton observations. The last column reports on the parameters derived from a joint fit of all four spectra with the latter model. Uncertainties in this table are given at 90 per cent confidence level.  $N_{\text{H}}$  is in units of  $10^{22} \text{ cm}^{-2}$  and solar abundances from Anders & Grevesse (1989) are assumed. The blackbody radius is calculated assuming a distance of 3 kpc (note that in the error calculation we did not consider the error in the distance). The blackbody flux fraction is calculated with respect to the absorbed 0.5–10 keV total flux. Fluxes are all absorbed and in units of  $10^{-10} \text{ erg cm}^{-2} \text{ s}^{-1}$ .

Parameters	2002 February	2003 January	2004 March	2004 July	Joint fit
$N_{\text{H}}$	$1.0^{+0.1}_{-0.1}$	$1.1^{+0.1}_{-0.1}$	$1.01^{+0.02}_{-0.04}$	$1.00^{+0.06}_{-0.01}$	$1.00^{+0.01}_{-0.01}$
$kT$ (keV)	$0.40^{+0.05}_{-0.03}$	$0.41^{+0.05}_{-0.05}$	$0.409^{+0.007}_{-0.001}$	$0.421^{+0.007}_{-0.004}$	$0.410^{+0.004}_{-0.002}$
BB radius (km)	$4.2^{+0.7}_{-0.5}$	$4.4^{+0.8}_{-0.5}$	$4.75^{+0.08}_{-0.06}$	$4.17^{+0.09}_{-0.07}$	$4.22^{+0.07}_{-0.02}$
BB flux (per cent)	$18^{+3}_{-1}$	$21^{+2}_{-2}$	$23.8^{+1.8}_{-0.2}$	$25.2^{+0.2}_{-0.1}$	$23.5^{+0.1}_{-0.1}$
$\Gamma$	$3.8^{+0.1}_{-0.1}$	$4.0^{+0.1}_{-0.2}$	$3.77^{+0.08}_{-0.02}$	$3.92^{+0.02}_{-0.02}$	$3.88^{+0.01}_{-0.01}$
Total flux 0.5–10 keV	$1.2^{+0.2}_{-0.1}$	$1.1^{+0.1}_{-0.1}$	$1.16^{+0.02}_{-0.01}$	$1.18^{+0.02}_{-0.02}$	$1.18^{+0.01}_{-0.01}$
Total flux 2–10 keV	$0.6^{+0.3}_{-0.4}$	$0.6^{+0.3}_{-0.3}$	$0.58^{+0.07}_{-0.06}$	$0.59^{+0.02}_{-0.03}$	$0.58^{+0.01}_{-0.01}$
$\chi^2_{\nu}$ (d.o.f.)	0.96 (88)	0.98 (90)	1.04 (210)	1.00 (210)	1.01 (590)

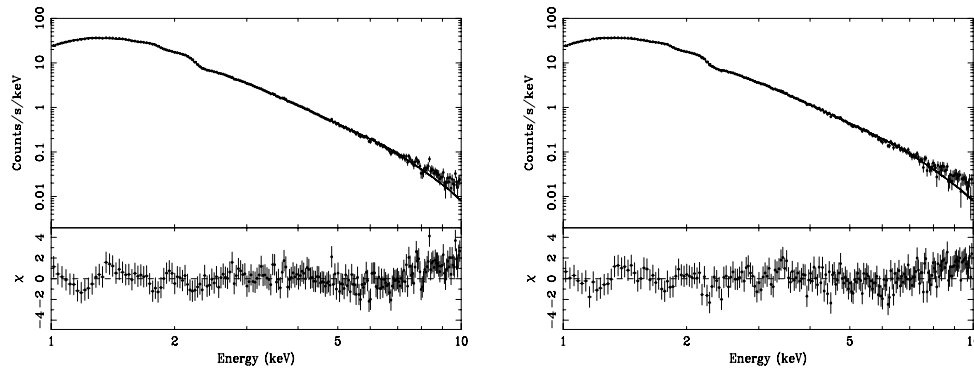


**Figure 3.** Phase-averaged spectra of the March (left-hand panel) and July (right-hand panel) XMM–Newton observations of 4U 0142+614 fitted with an absorbed blackbody plus a power-law model.

and 4); this would imply that only a fraction of the surface is emitting.<sup>4</sup>

The best-fitting parameters for the absorbed blackbody plus power-law model are only marginally ( $< 2\sigma$ ) variable between the observations (see Table 1; especially between the 2004 March and July pointings), and are all consistent with previous measurements (Israel et al. 1999; Paul et al. 2000; Juett et al. 2002; Patel et al. 2003). In order to shed light on possible marginal spectral variability in the 2004 observations, we have fitted all the spectra simultaneously with an absorbed blackbody plus power-law model, with all parameters tied between the spectra. Results are reported in Table 1 last column, and show that the spectrum does not display significant variability between the four observations. We also report in Fig. 4 on the contours plot for the photon index and absorption parameter for this the joint fit, showing that both parameters are relatively well constrained by this modelling. However, looking at the residuals

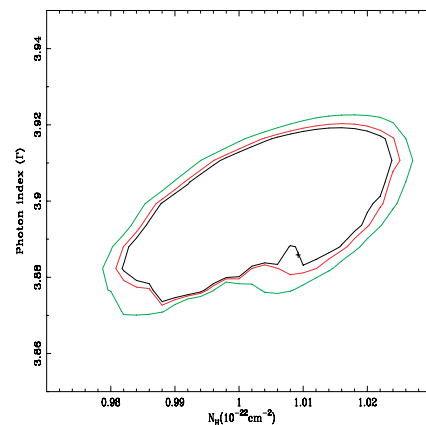


**Figure 4.** Contours plot of the photon index ( $\Gamma$ ) and the absorption parameter for the joint fit reported in Table 1. Confidence levels are from small to large: 1 $\sigma$ , 90 and 99 per cent. The small cross labels the values of the joint fit parameters reported in Table 1.

<sup>4</sup> Note that the measure of the emitting region can be strongly affected by the choice of the spectral model. For instance, in the case of cooling NSs, accounting for atmospheric effects would result in an emitting area larger than that inferred assuming blackbody emission (Perna et al. 2001). These atmospheric models are not directly applicable to AXPs, which are unlikely to be passive coolers. Nevertheless, the uncertainty on the spectral shape for the thermal component affects the determination of the emitting size.

we see a (not significant) excess in the residuals above 8 keV (see e.g. Fig. 3), probably due to the onset of the hard X-ray component (den Hartog et al. 2006; Kuiper et al. 2006; den Hartog et al. 2007). To shed light on this issue, we have attempted the fit of the 2004

March observation with the addition of the 25–250 keV *INTEGRAL* spectrum (see Section 3 for further details).

We also find some (not significant) deviations from the best-fitting model in the lower energy range (see Fig. 3) for the two deepest observations in 2004. However, we believe these deviations are due to both remaining calibration issues and/or, possibly, deviations in the interstellar medium (ISM) abundances from the (assumed) solar ones (see also Durant & van Kerkwijk 2006a).

We have performed a pulse-phase spectroscopy analysis for all the observations, but we report below only the two deeper observations in 2004, because previous *XMM-Newton* observations gave consistent results but with a smaller accuracy (see also Göhler et al. 2005) for the pulse phase spectroscopy of the 2003 January observation).

We have generated 10 phase-resolved spectra for each of the 2004 observations. Phase zero is arbitrarily set close to the start of the observations (MJD 53065.38674 and MJD 53210.30000 for the March and July observations, respectively) and with all phase bins of the same size. The choice of the number of intervals has been made a priori in order to have enough statistics in each phase-resolved spectra to detect, at a  $3\sigma$  confidence level, a cyclotron line with an equivalent width (EW)  $>30$  eV. This allows us to keep the number of trials to a minimum in case evidence for a cyclotron line is found.

The absorbed blackbody plus power-law model provides an excellent fits for all the 10 pulse phase-resolved spectra in both observations, either when leaving  $N_{\text{H}}$  free (see the second, third and fourth panels from top in Fig. 5) or when fixing it to the value obtained from the phase-averaged analysis (see last two panels in Fig. 5). In all the observations there is a similar spectral variability with phase, hence we show in Fig. 5 only the longer 2004 March observation. The phase-dependent photon index (as obtained from the fits with fixed absorption, see last panel of Fig. 5) shows deviations from a constant value with a significance of about  $4\sigma$ , while the blackbody temperature shows a  $3.3\sigma$  variability. The blackbody temperature seems to vary with phase in anticorrelation with the photon index, as also suggested by Patel et al. (2003). Note that Göhler et al. (2005) did not detect any phase-resolved blackbody temperature variability because of the much lower number of counts.

However, it should be noted that the  $N_{\text{H}}$  value we obtain from this modelling might be overestimated, since a lower value was found from fitting the ISM edges directly in the RGS data (Durant & van Kerkwijk 2006a) and by using other more physical, although yet less common, models (see Section 3 and Rea et al. 2007a).

No spectral features are detected in the phase-averaged and phase-resolved spectra of both the pn and RGS data (see also Juett et al. 2002, for the *Chandra* grating upper limits) of the two 2004 observations. In Table 2 we report the  $3\sigma$  upper limits of the EW of a Gaussian line with  $\sigma_{\text{line}} = 0$  (narrower than the pn instrumental energy resolution) and  $\sigma_{\text{line}} = 100$  eV. These are the deepest upper limits to date on the presence of lines in the spectra of an AXP. So far, the only evidence for an absorption line in an AXP, detected at a significance of  $\sim 3\sigma$ , was discovered by *BeppoSAX* (Rea et al. 2003; but see also Rea et al. 2005, 2007c) in an observation of the AXP 1RXS J170849.0–400910. This absorption line, tentatively interpreted as due to resonant cyclotron scattering, was observed at an energy of 8.1 keV, with a width of 0.2 keV and an EW of 0.8 keV. For 1RXS J170849.0–400910, the absorption line was observed when the source had a peculiar high X-ray flux and hard spectrum, while was not detectable during a subsequent observation (two years later) when 1RXS J170849.0–400910 was found at a lower flux level and with a softer X-ray spectrum (Rea et al. 2005, 2007c). Comparing our upper limits on the

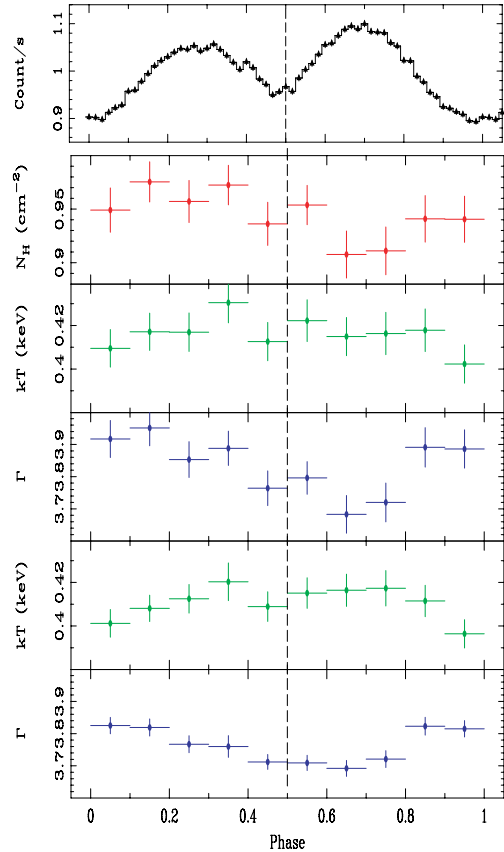


**Figure 5.** Top panel reports on the 0.3–10 keV pulse profile for the 2004 March observation. From top to bottom: second, third and fourth panels report on the spectral parameters of the pulse phase spectroscopy analysis for the 4U 0142+614 2004 March observations (see also Section 2.2) with the absorption parameter  $N_{\text{H}}$  free to vary. Last two panels correspond to phase-resolved spectral parameters with fixed  $N_{\text{H}} = 1 \times 10^{22} \text{ cm}^{-2}$ . Vertical dashed line is at phase 0.5 for clarity.

**Table 2.**  $3\sigma$  upper limits on the EW of a Gaussian line with width  $\sigma_{\text{line}} = 0$  (narrower than the pn instrumental energy resolution) and 100 eV, derived from the 2004 March *XMM-Newton* spectrum of 4U 0142+614.

Energy range (keV)	$\sigma_{\text{line}} = 0$ (eV)	$\sigma_{\text{line}} = 100$ (eV)
1–2	<4	<9
2–3	<4	<7
3–4	<12	<19
4–5	<16	<21
5–6	<25	<37
6–7	<46	<51
7–8	<88	<124
8–9	<405	<416
9–10	<527	<789

presence of lines in the spectrum of 4U 0142+614 (Table 2) with the 1RXS J170849.0–400910 line properties (Rea et al. 2003), we could have easily detected in the 4U 0142+614 0.3–9 keV spectrum any absorption or emission line with the same width and EW as observed in 1RXS J170849.0–400910.

### 3 MULTIBAND SPECTRAL MODELLING

The 4U 0142+614 X-ray spectrum has been discovered to have a hard X-ray component (Kuiper et al. 2006; den Hartog et al.

**Table 3.** Best-fitting parameters for the 1–250 keV spectral modelling of 4U 0142+614. Errors are at 90 per cent confidence level. Fluxes (if not otherwise specified) are unabsorbed and in units of  $10^{-10}$  erg cm $^{-2}$  s $^{-1}$ . RCS, BB, PL $_{\text{soft}}$  and log  $P_1$  fluxes are for the 0.5–10 keV energy band, while PL $_{\text{hard}}$  and log  $P_2$  fluxes refer to the 20–250 keV band. Total fluxes are in the 0.5–250 keV band.  $N_{\text{H}}$  is in units of  $10^{22}$  cm $^{-2}$ . The constant parameter, which accounts for the intercalibration, assumes XMM–Newton as a reference.

	BB + 2PL		RCS + PL		2 log-parabolas
$N_{\text{H}}$	$0.926^{+0.005}_{-0.005}$		$0.51^{+0.01}_{-0.01}$		$0.53^{+0.01}_{-0.01}$
Constant	1.2		0.86		0.6
$kT$ (keV)	$0.422^{+0.001}_{-0.002}$	$kT$ (keV)	$0.334^{+0.001}_{-0.002}$	$E_{P_1}$ (keV)	$1.37^{+0.03}_{-0.04}$
BB flux	$1.0^{+0.2}_{-0.1}$	$\tau_0$	$1.84^{+0.07}_{-0.03}$	$\beta_1$	$-3.21^{+0.12}_{-0.15}$
$\Gamma_{\text{soft}}$	$3.86^{+0.01}_{-0.01}$	$\beta_{\text{th}}$	$0.22^{+0.01}_{-0.02}$	log $P_1$ flux	$2.1^{+1.0}_{-0.9}$
$\Gamma_{\text{hard}}$	$0.8^{+0.1}_{-0.1}$	$\Gamma_{\text{hard}}$	$1.1^{+0.1}_{-0.1}$	$E_{P_2}$ (keV)	$200^{+80}_{-30}$
PL $_{\text{soft}}$ flux	$7.0^{+1.0}_{-1.0}$	RCS flux	$2.2^{+0.3}_{-0.7}$	$\beta_2$	$-0.6^{+0.1}_{-0.1}$
PL $_{\text{hard}}$ flux	$1.7^{+0.4}_{-1.2}$	PL $_{\text{hard}}$ flux	$1.5^{+0.8}_{-0.9}$	log $P_2$ flux	$2.0^{+1.2}_{-1.0}$
Total absolute flux	$2.6^{+0.4}_{-0.5}$		$3.0^{+0.1}_{-0.4}$		$3.3^{+0.2}_{-1.0}$
Total flux	$8.4^{+0.9}_{-0.3}$		$4.1^{+0.8}_{-0.5}$		$4.4^{+1.1}_{-1.0}$
$\chi^2_{\nu}$ (d.o.f.)	1.09 (225)		1.06 (225)		0.82 (225)

2007). Rea et al. (2007a) applied several models to the 0.5–250 keV 4U 0142+614 spectrum in order to model the emission of this source across this large energy range, using simultaneous observations performed in 2005 July with *Swift* XRT (0.5–8 keV) and *INTEGRAL* (25–250 keV; den Hartog et al. 2007). Here we use the latter *INTEGRAL* spectrum fitting it together with our 2004 March XMM–Newton observation (being the longest one). This multiband fitting is performed in order to (i) assess the presence of an hard component in the 8–10 keV XMM–Newton spectrum of 4U 0142+614 (see Fig. 3) and (ii) test whether the spectral parameters derived in Rea et al. (2007a), are consistent with those derived from the higher XMM–Newton statistics and larger energy band (we used here the pn in the 1–10 keV energy range).

We note that, at variance with what has been done in Rea et al. (2007a), these observations are not simultaneous. However, the soft X-ray spectrum shows only a very modest variability between the *Swift* XRT observation performed in 2005 July (simultaneous to the *INTEGRAL* observation we use here) and the XMM–Newton observations we report here. We then tentatively rely on the stability of the hard X-ray spectrum and try to fit the overall spectrum assuming that the source is in the same emission state during both the XMM–Newton and the *INTEGRAL* observations.

We fit the 1–250 keV spectrum with: one absorbed blackbody plus two power laws, an absorbed resonant cyclotron scattering model plus a power law and two absorbed log-parabolas (Table 3; see Rea et al. 2007a, for further details on these models).

We find that all these models, remove the excess in the >8 keV residuals (not significant though) found in the XMM–Newton spectrum when fitted with an absorbed blackbody plus a single power law (see Fig. 3 and Table 1). We then conclude that this excess in the residuals is indeed due to the presence of the hard X-ray component. Furthermore, the spectral parameters we find for the three best-fitting models are consistent (within  $3\sigma$  statistical accuracy) with those reported by Rea et al. (2007a) using the *Swift* XRT spectrum, with lower statistics and smaller energy coverage. We note that the constant parameter in the fitting of the two log-parabolas is slightly smaller than the range of values that the cross-calibration between XMM–Newton and *INTEGRAL*, should take. This might be either a hint of the fact that the second log-parabola can barely take into account the 8–10 keV part of the spectrum which was missing

in the *Swift* XRT spectrum, or simply a statistical fluctuation. A simultaneous observation of 4U 0142+614 with XMM–Newton and a longer *INTEGRAL*, exposure might shed light on this issue.

#### 4 DISCUSSION

We reported here on the timing and spectral analysis of four XMM–Newton observations of the AXP 4U 0142+614 performed from 2002 to 2004, representing the deepest X-ray observations on this source performed to date.

The pulse profile of 4U 0142+614 is double peaked in the soft X-rays, and largely variable as a function of energy; we also detect an increase with energy of the fundamental pulsed fraction component (see also hints for this increase in Israel et al. 1999; Paul et al. 2000; Göhler et al. 2005). Furthermore, 10 yr of *RXTE* monitoring also revealed the pulse profile to be very variable in time, possibly related to the presence of glitches (Dib et al. 2007; but see also Morii et al. 2005).

The presence of two distinct peaks in the phase profile of 4U 0142+614 suggests that the emission might be concentrated in two regions on the star surface. Since the two maxima are offset by half a phase cycle, the emission regions must be located antipodally on the surface of the star. In a ‘standard’ cooling NS, such a geometry of the emission regions would be naturally produced by a (core-centred) dipolar magnetic field. In fact, since heat flows preferentially along the magnetic field lines, in this scenario the polar regions (where the field lines are more closely packed) turn out to be hotter than the equatorial belt. On the other hand, for such configurations, the pulsed fractions are low, the more when gravity effects are accounted for (e.g. Page 1995; Perna et al. 2000; Dedeo, Psaltis & Narayan 2001). The very high pulsed fraction of the hard ( $\gtrsim 100$  keV; Kuiper et al. 2006; den Hartog et al. 2007) photons may be explained if they are produced in regions high up in the magnetosphere, where no relativistic effects are expected to wash out the pulsed emission. This might also tentatively explain the increase of the pulsed fraction with energy, in particular between the band dominated by the thermal component, and that dominated by the power law. However, much more detailed theoretical models are needed to fully interpret this phenomenon. In fact, it is unlikely that magnetars are passive coolers in which the surface temperature

distribution is solely determined by the large-scale field topology. As stressed by Thompson, Lyutikov & Kulkarni (2002), portions of the star surface are heated by the returning currents which flow into a ‘twisted’ magnetosphere, and this may be a possible explanation for the presence of hotter regions on the star surface. It has been recently suggested (Thompson et al. 2002; Lyutikov & Gavriil 2005; Fernandez & Thompson 2007) that the mechanism responsible for the formation of the 0.1–10 keV spectrum of AXPs and SGRs is cyclotron resonant upscattering of soft ( $\sim 0.5$  keV) thermal photons produced at the star surface by electrons (or pairs) which fill the (twisted) magnetosphere. Currents are mainly concentrated towards the magnetic equator, and this, as the Monte Carlo simulations of Fernandez & Thompson (2007) show, makes the emission pulsed even if primary thermal photons are produced uniformly at the star surface. We performed some preliminary calculations with a Monte Carlo code (Nobili et al., in preparation) in order to check if the increase of the pulsed fraction with energy is qualitatively reproduced by the resonant scattering model. For instance, assuming that the star is an orthogonal rotator seen at an angle  $\sim 90^\circ$  with respect to the rotation axis, we find that the low-energy (0.5–2 keV) light curve should be double peaked while, at higher energies (7–10 keV), the secondary peak tends to disappear and the pulsed fraction increases.

At variance with what has been recently found for a few other AXPs (e.g. 1RXS J170849.0–400910, 1E 1048.1–5937 and 1E 2259+586; Mereghetti et al. 2004; Woods et al. 2004; Rea et al. 2005), these very deep X-ray observations of the AXP 4U 0142+614 find the source stable in flux and spectral shape. However, spectral and flux variability are expected to be connected with the AXP bursting activity, as e.g. detected for 1E 2259+586 (Kaspi et al. 2003; Woods et al. 2004). Hence, the recent bursting activity of 4U 0142+614 (Gavriil et al. 2007; Kaspi, Dib & Gavriil 2006) should have probably disturbed its steady emission state, and the source might have recently enhanced its flux and hardened its spectral shape.

Furthermore, we put very strong upper limits on the presence of X-ray lines in the spectrum of this AXP, either of resonant cyclotron or atmospheric nature, the deepest upper limits for an AXP to date. This is a further confirmation that the X-ray spectral lines, possible due to proton cyclotron scattering, or to absorption by the NS atmosphere, are either very weak, or not present at all (e.g. suppressed by QCD processes; Ho & Lai 2003; van Adelsberg & Lai 2006) in the spectra of AXPs, and probably also of SGRs.

## ACKNOWLEDGMENTS

This paper is based on observations obtained with *XMM-Newton*, an ESA science mission with instruments and contributions directly funded by ESA Member States and the USA (NASA). NR is supported by an NWO Post-doctoral Fellowship, and thanks Lucien Kuiper for useful comments, and Vicky Kaspi and Marjorie Gonzalez for useful discussion about the pulsed fraction variability of this source. SZ thanks PPARC for financial support. We thank the referee for his/her very useful suggestions.

## REFERENCES

van Adelsberg M., Lai D., 2006, *MNRAS*, 373, 1495  
 Alpar M. A., 2001, *ApJ*, 554, 12  
 Anders E., Grevesse N., 1989, *Geochim. Cosmochim. Acta*, 53, 197  
 Baring M. G., Harding A. K., 1998, *ApJ*, 507, L55

Camilo F., Kaspi V. M., Lyne A. G., Manchester R. N., Bell J. F., D’Amico N., McKay N. P. F., Crawford F., 2000, *ApJ*, 541, 367  
 Camilo F., Ransom S. M., Halpern J. P., Reynolds J., Helfand D. J., Zimmerman N., Sarkissian J., 2006, *Nat*, 442, 892  
 Chatterjee P., Hernquist L., Narayan R., 2000, *ApJ*, 534, 373  
 Dedeo S., Psaltis D., Narayan R., 2001, *ApJ*, 559, 346  
 den Hartog P. R., Hermsen W., Kuiper L., Vink J., in’t Zand J. J. M., Collmar W., 2006, *A&A*, 451, 2  
 den Hartog P. R., Kuiper L., Hermsen W., Rea N., Durant M., Stappers B., Kaspi V. M., Dib R., 2007, *Ap&SS*, 308, 647  
 den Herder J. W. et al., 2001, *A&A*, 365, L7  
 Dib R., Kaspi V. M., Gavriil F. P., 2007, *Ap&SS*, 308, 487  
 Duncan R. C., Thompson C., 1992, *ApJ*, 392, L9  
 Durant M., van Kerkwijk M. H., 2006a, *ApJ*, 650, 1082  
 Durant M., van Kerkwijk M. H., 2006b, *ApJ*, 652, 576  
 Fernandez R., Thompson C., 2007, *ApJ*, 660, 615  
 Forman W., Jones C., Cominsky L., Julien P., Murray S., Peters G., Tananbaum H., Giacconi R., 1978, *ApJS*, 38, 357  
 Gavriil F. P., Kaspi V. M., 2002, *ApJ*, 38, 357  
 Gavriil F. P., Dib R., Kaspi V. M., Woods P. M., 2007, *ATEL # 993*  
 Göhler E., Wilms J., Staubert R., 2005, *A&A*, 433, 1079  
 Ho W. C. G., Lai D., 2003, *MNRAS*, 338, 233  
 Hulleman F., van Kerkwijk M. H., Kulkarni S. R., 2000, *Nat*, 408, 689  
 Israel G. L., Mereghetti S., Stella L., 1994, *ApJ*, 346, L25  
 Israel G. L. et al., 1999, *A&A*, 346, 929  
 Jansen F. et al., 2001, *A&A*, 365, L1  
 Juett A. M., Marshall H. L., Chakrabarty D., Schulz N. S., 2002, *ApJ*, 568, L31  
 Kaspi V. M., Gavriil F. P., Woods P. M., Jensen J. B., Roberts M. S. E., Chakrabarty D., 2003, *ApJ*, 588, L93  
 Kaspi V. M., Dib R., Gavriil F., 2006, *ATEL # 794*  
 Kern B., Martin C., 2001, *IAU Circ.*, 7769, 2  
 Kuiper L., Hermsen W., den Hartog P. R., Collmar W., 2006, *ApJ*, 645, 556  
 Lyutikov M., Gavriil F. P., 2005, *MNRAS*, 368, 690  
 Mason K. O. et al., 2001, *A&A*, 365, L36  
 Mereghetti S., Tiengo A., Stella L., Israel G. L., Rea N., Zane S., Oosterbroek T., 2004, *ApJ*, 608, 427  
 Morii M., Kawai N., Shibasaki N., 2005, *ApJ*, 622 544  
 Page D., 1995, *ApJ*, 442, 273  
 Patel S. et al., 2003, *ApJ*, 587, 367  
 Perna R., Heyl J., Hernquist L., 2000, *ApJ*, 541, 344  
 Perna R., Heyl J. S., Hernquist L., Juett A. M., Chakrabarty D., 2001, *ApJ*, 557, 18  
 Paul B., Kawasaki M., Dotani T., Nagase F., 2000, *ApJ*, 537, 319  
 Rea N., Israel G. L., Stella L., Oosterbroek T., Mereghetti S., Angelini L., Campana S., Covino S., 2003, *ApJ*, 586, L65  
 Rea N., Oosterbroek T., Zane S., Turolla R., Mendez M., Israel G. L., Stella L., Haberl F., 2005, *MNRAS*, 361, 710  
 Rea N. et al., 2007a, *ApJ*, 661, L65  
 Rea N., Zane S., Lyutikov M., Turolla R., 2007b, *Ap&SS*, 308, 61  
 Rea N., Israel G. L., Oosterbroek T. et al., 2007c, *Ap&SS*, 308, 505  
 Strüder L. et al., 2001, *A&A*, 365, L18  
 Thompson C., Duncan R. C., 1993, *ApJ*, 408, 194  
 Thompson C., Duncan R. C., 1995, *MNRAS*, 275, 255  
 Thompson C., Duncan R. C., 1996, *ApJ*, 473, 322  
 Thompson C., Lyutikov M., Kulkarni S. R., 2002, *ApJ*, 574, 332  
 Turner M. J. L. et al., 2001, *A&A*, 365, L27  
 van Paradijs J., Taam R. E., van den Heuvel E. P. J., 1995, *A&A*, 299, L41  
 White N. E., Mason K. O., Giommi P., Angelini L., Pooley G., Branduardi-Raymont G., Murdin P. G., Wall J. V., 1987, *MNRAS*, 227, 545  
 Wilson C. A., Dieters S., Finger M. H., Scott D. M., van Paradijs J., 1999, *ApJ*, 513, 464  
 Woods P., Thompson C., 2006, in Lewin W., van der Klis M., eds, *Compact Stellar X-ray Sources*. Cambridge Univ. Press, Cambridge  
 Woods P. M. et al., 2004, *ApJ*, 605, 378

This paper has been typeset from a  $\text{\TeX}/\text{\LaTeX}$  file prepared by the author.